Physiologic left heart performance of a fluid-structure interaction model of the human heart

Marshall Davey[1], Charles Puelz[5], Simone Rossi[2], Margaret Anne Smith[2], David Wells[2], and Boyce E. Griffith[2,3,4]
Departments of [1]Bioinformatics and Computational Biology, [2]Mathematics, [3]Applied Physical Sciences, and [4]Biomedical Engineering, University of North Carolina at Chapel Hill, and [5]Pediatrics-Cardiology, Baylor College of Medicine

Introduction

Cardiovascular disease is the leading cause of death in the United States, and the estimated cost associated with heart diseases in the U.S. alone is over $200 billion per year [1]. This work aims to develop a comprehensive heart model that couples realistic descriptions of the biomechanics of the heart and its valves to the fluid dynamics of the blood.

Numerical Approach

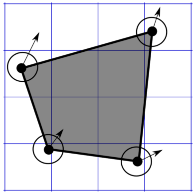

$$\rho\frac{\mathrm{D}\mathbf{u}}{\mathrm{D}t}(\mathbf{x},t) = -\nabla p(\mathbf{x},t) + \mu\nabla^2\mathbf{u}(\mathbf{x},t) + \mathbf{f}(\mathbf{x},t),$$

$$\nabla\cdot\mathbf{u}(\mathbf{x},t) = 0,$$

$$\mathbf{f}(\mathbf{x},t) = \int_U \nabla_{\mathbf{X}}\cdot\mathbb{P}(\mathbf{X},t)\,\delta(\mathbf{x}-\boldsymbol{\chi}(\mathbf{X},t))\,\mathrm{d}\mathbf{X} - \int_{\partial U}\mathbb{P}(\mathbf{X},t)\,\mathbf{N}(\mathbf{X})\,\delta(\mathbf{x}-\boldsymbol{\chi}(\mathbf{X},t))\,\mathrm{d}A(\mathbf{X}),$$

$$\frac{\partial\boldsymbol{\chi}}{\partial t}(\mathbf{X},t) = \int_\Omega \mathbf{u}(\mathbf{x},t)\,\delta(\mathbf{x}-\boldsymbol{\chi}(\mathbf{X},t))\,\mathrm{d}\mathbf{x} = \mathbf{u}(\boldsymbol{\chi}(\mathbf{X},t),t)$$

Figure 1: The immersed finite element/finite difference method [2] through the **IBAMR** software package defines the dynamics and stresses of a finite element description of a structure immersed in and moving with a material defined by the incompressible Navier-Stokes equations.

Anatomy Construction

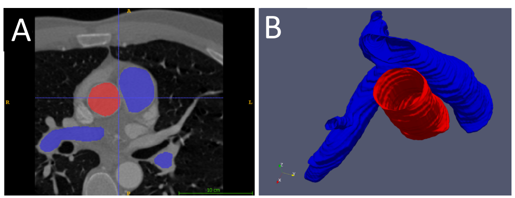

Figure 2: The model was primarily constructed using CT data (**A**) from a healthy human subject. The process, called segmentation, results in surface representations (**B**) that are thickened to physiologic values.

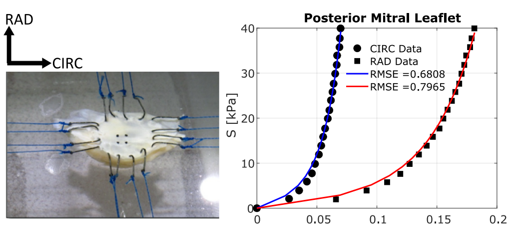

Figure 3: The materials of the heart are highly anisotropic because of the myofiber alignment in the myocardium and the collagen alignment in the valves. The material parameters are derived from tissue tensile analysis experiments aligned with the mean fiber orientations (**left**, adapted from Pham et al. [3]) which result in stress-strain curves (**right**) used for constitutive model fitting.

Model Description

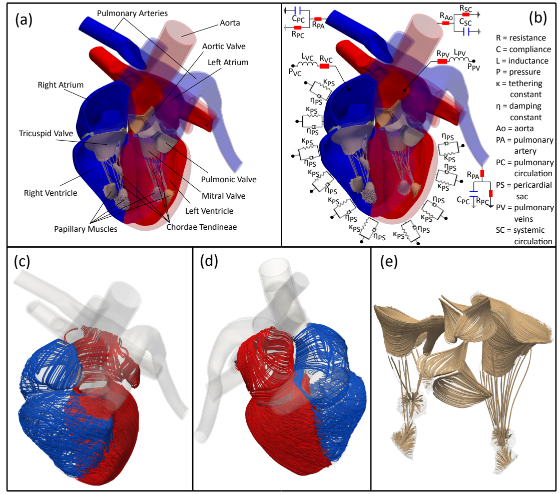

Figure 4: The heart geometry **(a)** captures the major features of the heart, including all four valves, with appropriate boundary conditions for the circulation and pericardial constraint **(b)**. The fiber fields in the heart that characterize the axes of anisotropy are defined throughout the myocardium **(c-d)** and the valves **(e)**.

Left Ventricular Dynamics

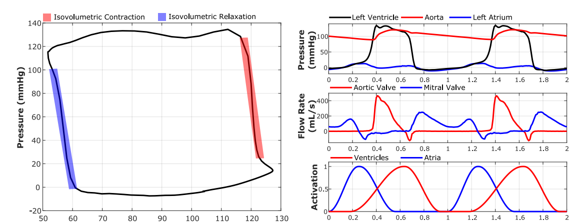

Figure 5: The left ventricular pressure-volume relation (**left**) captures characteristics of the cardiac cycle, including the isovolumetric phases and the stroke volume. The right panels show pressure, flow rate, and activation waveforms for two successive cardiac cycles.

	ESV (mL)	EDV (mL)	SV (mL)	EF	CO ($\mathrm{L{\cdot}min^{-1}}$)
Model	127.30	51.73	75.57	0.59	4.5
Target [4]	120	50	70	0.58	4.2

Table 1: Left ventricular performance metrics: ESV = end systolic volume, EDV = end diastolic volume, SV = stroke volume, EF = ejection fraction, and CO = cardiac output, which is computed from the SV and the heart rate (60 BPM).

Cycle Visualization

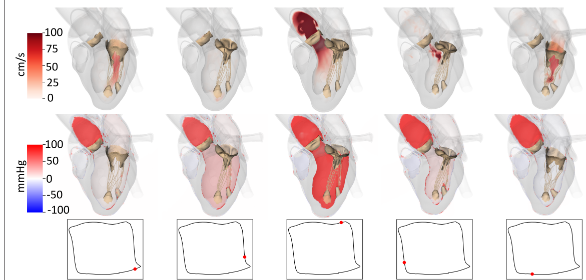

Figure 6: Blood velocity magnitude (**top**) and pressure (**middle**) at points of the cardiac cycle illustrated by the left ventricular pressure-volume relation (**bottom**). The valves act appropriately as pressure gates between the chambers and the vessels throughout the cycle.

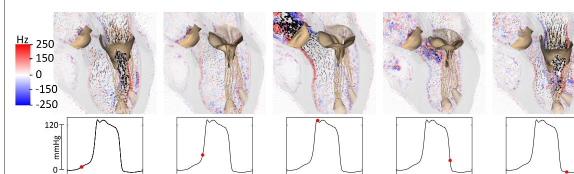

Figure 7: Blood velocity vectors (**top**) and vorticity (**top**) at points of the cardiac cycle illustrated by the left ventricular pressure waveform (**bottom**).

Frank-Starling Response

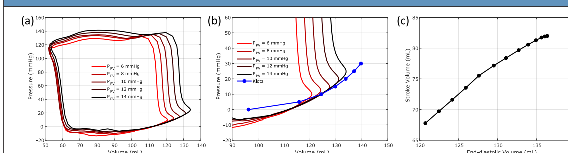

Figure 8: (a) Left ventricular pressure-volume relations over consecutive cycles with increasing atrial preload mimicking in vivo vena cava occlusion studies. (b) End-diastolic portion of the pressure-volume relation with the Klotz relation [5] superimposed illustrating differences in passive versus active filling dynamics. (c) Left ventricular function curve demonstrating the Frank-Starling relation.

Acknowledgments and Citations

We gratefully acknowledge funding from the NIH (Awards R01HL117063, U01HL143336, and R01HL157631) and NSF (Awards OAC 1450327, OAC 1652541, OAC 1931516, and CBET 1757193).

References:

1. `https://www.cdc.gov/heartdisease/facts.htm`.
2. Griffith, BE and Luo, X. *Int J Numer Meth Biomed Eng* 33(12), 2017.
3. Pham, T et al. *Acta Biomater* 45, 2017.
4. Hall, JE. Guyton and Hall Textbook of Medical Physiology, 13e, 2016.
5. Klotz, S et al. *Am J Physiol Heart Circ Physiol* 291(1), 2006.